Modular Soft Robotic Actuators from Flexible Perforated Sheets

Nicholas Pagliocca[1,†], *Mitja Trkov*[1,*], *Behrad Koohbor*[1,2,*]

1. Department of Mechanical Engineering, Rowan University, 201 Mullica Hill Rd., Glassboro, NJ 08028, USA
2. Advanced Materials and Manufacturing Institute (AMMI), Rowan University, 201 Mullica Hill Rd., Glassboro, NJ 08028, USA
†. Presently at the Department of Electrical and Computer Engineering, University of Michigan
*. Corresponding Authors: trkov@rowan.edu (M. Trkov), koohbor@rowan.edu (B. Koohbor)

Keywords: Soft Robotics, Mechanical Metamaterial, Actuators, Modular Robots, Architected Structures

Soft robotic actuators can be designed to achieve complex and tailored motions while simultaneously leveraging their compliance to interact with complex and often delicate environments. Mechanical metamaterials reveal a route to customizable deformations, force exertion, and mechanical energy efficiency attainable by careful arrangement of local geometric features. In this study, modular soft robotic actuators are developed from soft elastomers and flexible thermoplastic sheets of various unit cell designs. We focus our efforts on center-symmetric perforated sheets, which are formed into flexible cylindrical skins that surround the soft inflatable actuators. Our results demonstrate the influence of perforation geometry on the spatial stiffness of the reinforcement structure and the proposed actuators' response through several investigations. We demonstrate that the free-boundary displacement, maximal force exertion, and mechanical energy efficiency of extensile actuators are dependent on a change of deformation mode in the meso-structure. The spatial stiffness concept is extended to develop soft robotic actuators that can bend, twist, and perform hybrid motions, such as simultaneous bending and twisting. Multi-segment soft robotic arms are also developed from the aforementioned actuators. Investigations in this study provide a step towards the development of highly customizable and programmable soft robotic actuators for various applications.

Author Manuscript

This is the author manuscript accepted for publication and has undergone full peer review but has not been through the copyediting, typesetting, pagination and proofreading process, which may lead to differences between this version and the Version of Record. Please cite this article as doi: 10.1002/adem.202300583.

This article is protected by copyright. All rights reserved

1. Introduction

Soft robotic actuators rely on controlled deformations of their compliant bodies to maneuver in environments and manipulate objects. The intrinsic compliance of soft robotic systems has lent to their use in applications such as environmental exploration,[1] human-machine interactions,[2-4] material handling,[5, 6] and many others. Often drawing inspiration from biology, soft robotic actuators realize their deformation-driven responses by leveraging structural anisotropy and reinforcement materials such as fibers.[7-9] Common motions studied in the literature include contraction, extension, bending, and twisting.[7, 8, 10, 11] Hybrid motions, such as the combination of extension, bending and twisting can be achieved by rational placement of fibers,[8] or by using other novel approaches like bubble casting methods.[12] The continued exploration and advancement of materials and structures used in soft robotic actuators may lead to novel or optimized mechanical responses and actuation modes, which can be vital to unlocking the full potential of soft robotics.

Perforated structures have drawn notable attention as a medium to program motions of soft robotic systems of various global morphologies. Often, these methodologies are cited as kirigami-inspired, as they leverage cutting and manipulating reinforcement elements.[13] Some examples of perforation styles of planar structures include diamond,[14] circular,[15] center-symmetric rotating squares,[16] triangles,[17, 18] stars,[19] hierarchical squares,[20] and random cuts and slits.[21] By altering the local morphology of unit cells, structure stiffness can be locally modified or tuned. Specifically, such structures can be used to engineer lattices that can achieve complex meso- and macro-mechanical motions. An example of modulating the spatial stiffness of a 2D perforated structure was shown in the work of Yao *et al*.[22], where the authors developed a Poisson's ratio-based unit cell optimization method that allowed for the macroscale design of deformations in structures. Within the domain of metamaterials research, it has been proposed that these structures can be designed and optimized to achieve a prescribed motion as flexible skin in a tubular configuration with motion types that include bending, expansion, etc.[23] Several tubular configurations from 2D mechanical metamaterials have been developed in the literature,[24-29] which may also serve as promising candidates for such programmed deformations. Hedayati *et al*.[29] presented several patterns using cell-density gradients to deform into shapes upon external tensile and compressive loads such as an hourglass, a barrel, and a vase. Cylindrical structures fabricated with the aforementioned patterns can serve as actuators achieving twist and bending motions using pores instead of sleeves.[30, 31] Naturally, the notion of an internal structural pattern derived from pours can also be extended to other soft actuators and machines of high utility.[32, 33] The recurring theme in all aforementioned studies is that the investigation and exploitation of the so-called mechanical metamaterials have opened the door to the development of the next generation of soft robotic

This article is protected by copyright. All rights reserved

Author Manuscript

systems, which can greatly benefit from parallel explorations in materials and modeling, to which this paper complements.

Patterned flexible sleeves with planar auxetic unit cells have recently been considered to program deformations into tubular soft robotic actuators. For example, Sedal *et al*.[34, 35] developed sleeves composed of representative auxetic elements -unit cells with negative Poisson's ratio- that act as a reinforcement framework. Aside from developing analytical models, their reports provide detailed discussions of bending and expansion functionalities in such soft actuators. Others have developed re-entrant compliant structures, *e.g.*, tiled auxetic cylinders, for soft robots emphasizing that such structures can passively conform to mediums they interact with as a consequence of their complex but tunable mechanics.[36] Several research groups have recently leveraged ideas from kirigami to program complex motions and functionalities into soft robotic actuators.[13, 37-41]. Kirigami skins have also found use in sensory applications as an emerging technology in soft robotics.[42] Most important to these previous research works is the development of soft robotic actuators with programmable shapes and mechanical responses, both of which are attainable with the careful and rational placement of voids in a soft actuator's reinforcement material. Jin *et al*.[13] presented the design of kirigami balloons that are able to extend, bend, twist, and achieve hybrid motions, *e.g.*, bending and twisting, and as a result were able to achieve shape and path matching by finite element analyses coupled with in-the-loop optimization.

The results of Jin *et al*.[13] and Sedal *et al*.[34], in particular, demonstrate the utility of architected materials in the development of soft robotic actuators with complex motions and shape matching capabilities. Structures with such programmed motions could be further explored to develop modules with compliant interfaces to achieve extension, bending, twisting, and hybrid motions. A limitation of the aforementioned literature is that the investigations are limited to developing structures and approaches to enable new and tailored motions. However, previous research has not investigated the actuators' capacity to interact with an environment, force exertion, and determine how efficient they are in relation to their meso mechanics.

The present paper contributes to the existing research on soft actuators by developing a framework for soft actuator design using architected structures. The presented approach uniquely focuses on the meso-mechanics of the unit cells in a lattice structure, namely flexible perforated sheets, whose local deformations govern the overall deformation of an actuator at macroscales. As such, we experimentally investigate the mechanics of pneumatic soft robotic actuators that are wrapped in a flexible perforated skin. We demonstrate and characterize the deformation-based actuators' modalities and mechanical performance and efficiency. The flexible perforated skin is designed as a planar center-symmetric perforated structure. We use 3D-printed thermoplastic polyurethane (TPU) to develop these perforated sheets, with the intention of presenting a simplified

This article is protected by copyright. All rights reserved

Author Manuscript

and scalable fabrication process. Extensile actuators are characterized in three tests including free-boundary displacement, with a confined upper-boundary, and while transporting a fixed mass. We select these metrics as they represent free-form motion, maximal force capacity, and enable efficiency measurement. Unit cells are selected to investigate the role of the meso-structure of the architected materials on macroscale (global) performance. Our fabrication process is extended to realize simple designs of bending, twisting, and hybrid twisting-bending actuators similar to those reported in Jin *et al*.[13] These actuators can serve as individual modules for constructing soft robotic systems with programmable characteristics. In addition, they provide an enhanced envelope of attainable motions due to their spatially tailorable stiffness, which is the result of the local unit cell design. Last, the modules are used to construct a multisegmented actuator to demonstrate the actuators' functionality and utility that contribute to the advancements in the domain of modular soft robotics.

2. Results

2.1. Multiscale Mechanical Response of Uniform Flexible Sheets

The actuators investigated herein were composed of an inflatable silicone rubber inner tube that was wrapped inside a planar perforated sheet additively manufactured from TPU using the fused filament fabrication (FFF) method. Before embarking on further details regarding the actuator design, it is important to understand the multiscale mechanics of the reinforcement material as it governs the actuators' mechanical deformations. Traditionally, researchers have focused on perforated sheets to achieve large negative Poisson's ratios (auxeticity) and/or tailored responses via gradient designs using various experimental and computational approaches.[16-22] Focusing on center-symmetric perforated structures herein, we leverage their tailorable local geometries to modulate spatial stiffness and Poisson's ratio for controlled mechanical deformations.

The primary unit cells explored in the development of the proposed soft robotic actuators are presented in **Figure 1(a,b)**. Geometric parameters, a and b, define the dimensions of the horizontal and vertical perforations, respectively. Their ratio is described by the Aspect Ratio (*A.R.*). The geometric parameter s defines the dimension of the wall segment. In all unit cells examined in this study, the cell edge length, L, was kept constant at 10 mm. The ratio, s/L defines the Inter-cell Spacing (*I.S.*). The mechanical response of the unit cells can be controlled by adjusting these geometric parameters and their non-dimensional relationships. It is important to note that changing the perforation design changes a unit cell's relative density.[43] When the density is varied along one axis, it will produce a cell-density gradient, which has been the topic of research in the materials domain with demonstrated improvements in the mechanical performance of the structure.[44, 45]

Author Manuscript

This article is protected by copyright. All rights reserved

At local (meso) scale, there is a strain-dependent variation in mechanical compliance that is induced by the rotation of the solid portions of the unit cells. Specifically, unit cells with a high *A.R.* and low *I.S.* experience large cell rotations, while those with a low *A.R.* and high *I.S.* experience insignificant rotation. For in-plane uniaxial loading, these rotations are commonly used to control the Poisson's ratio of the structure as previously discussed. However, the soft robotic actuators in this research will experience a complex state of multi-axial stress upon pressurization, not characteristic of their in-plane response. As such, further discussions of global auxetic responses of these structures are avoided herein.

We demonstrate the role of perforation geometry on local structure response by studying the full-field deformation using 2D digital image correlation (DIC). Axial strain fields, ϵ_{yy}, are presented at increasing global axial strains, *e*, in **Figure 1(c,d)** for structures with *A.R.*=5, *I.S.*=0.1 and *A.R.*=1, *I.S.*=0.2, respectively. The strain-dependent cell rotations and eventual saturation, as discussed in Pagliocca *et al.*,[16] are elucidated by the response of the unit cell in **Figure 1(c)**. Differences in the mechanical response of the unit cells are also highlighted by the heterogeneous strain distribution approaching the hinges as shown in **Figure 1**. Specifically, as the unit cell is increasingly elongated, the strain intensity increases at and in the vicinity of the hinges. Prior to this point, strain in the unit cells is low throughout the entire region of interest. These results differ from those of unit cells with low *A.R.* shown in **Figure 1(d)**, whose strain accumulations are more uniform spatially, and whose mechanical response is stiffer than that of cells allowing cell rotation. The saturation of rotation and inevitable accumulation of strain in the unit cell in **Figure 1(c)** leads to a transition of deformation mode, leading to a stretch-dominated mode over the rotation-dominated deformation mechanism discussed earlier. The mode transition discussed above is governed by the interplay of local strain fields and their effect on cell rotation.[46] Controlling the rate of local cell rotations and strains upon pressurization and loading is at the core of the methodology discussed in this work. We directly utilize the unit cells investigated in **Figure 1** in the development of actuators of various forms and functions in the following discussions. Further details and results regarding the methods, stress-strain response, and Poisson's ratio of the structures presented in **Figure 1**, and a cell-density gradient design discussed in the forthcoming section are provided in the **Supplementary Information** document.

Author Manuscript

This article is protected by copyright. All rights reserved

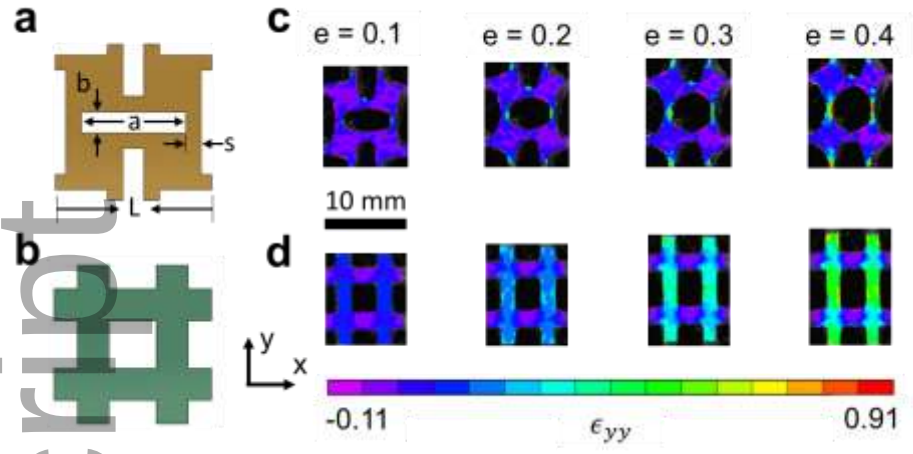


Figure 1: Unit cell designs utilized in the development of soft robotic actuators and their local mechanical response. (a) Shows a unit cell with an *A.R.* of 5 and an *I.S.* of 0.1. (b) Shows a unit cell with an *A.R.* of 1 and an *I.S.* of 0.2. Axial strain, ϵ_{yy}, contour maps are presented in (c) and (d), for the cell geometries in (a) and (b), respectively, showing the strain fields at various global axial strains, *e*.

2.2. Extensile Actuator Design and Fabrication

Soft robotic actuators were designed and fabricated to achieve tailored extensile motions with reinforcement structures developed from the unit cells presented in **Figure 1**, as shown by renderings in **Figure 2(a-c)**, and a gradient structure outlined in **Figure 2(d)**. The actuators' heights, *h*, were 110 mm. A longitudinal cross-section view of the actuator shown in **Figure 2(b)** is presented in **Figure 2(c)**. The end cap height, h_{cap}, was 10 mm, and the inlet diameter, D_{in}, was 2 mm. The inner radius, R_i, middle radius, R_m, and outer radius, R_o, were 10.21 mm, 13.34 mm, and 14.43 mm, respectively. The sheet presented in **Figure 2(d)** was developed in previous work by the authors and exhibits a near-zero in-plane Poisson's ratio when loaded in axial tension.[16] Here, we intentionally re-purpose the design to demonstrate the utility of spatially variable cell density in various actuation boundary conditions. All sheets were designed with a 9×9 array of unit cells with 10 mm tabs at each end.

The inner cylinders were cast in a two-step process using Ecoflex 00-50 (Smooth-On, Inc., Macungie, PA, USA) silicone rubber material. The reinforcement layers were additively manufactured using FFF from TPU and formed into cylinders by a joining process that leverages the thermoplastic properties of the material, allowing for the thermally assisted seamless joining of the interface. Specifically, we formed the sheet around a cylinder and used a soldering tool to fuse the ends of the sheet together. We note that the seam at the sheets' joint was the weakest region of the actuator. Therefore, while not investigated in this work, it is anticipated that failure would most

This article is protected by copyright. All rights reserved

Author Manuscript

likely initiate from these areas at high internal pressures. The cylinders were slid over the inner silicone tube to complete the construction. Cylindrical structures were not cast into the walls of the inner tube to allow unconstrained local cell rotations. As such, we acknowledge the presence of friction between the inner silicone core and the metamaterial sleeves upon inflation. While the aforementioned forming process is not as elegant as printing the reinforcement sheet in a single step, it can be amendable to large-scale processing and production by cutting flat sheets of thermoplastic material and rapidly fusing the ends together in an automated forming process. The methodology presented here was developed in an effort to improve upon the fabrication times of the methods proposed in the literature. For example, Sedal *et al*.[34] fabricated tubes with auxetic elements using stereolithography printing and associated post-processing, whereas Jin *et al*.[13] first laser cut a kirigami pattern into polyester sheets and used an adhesive to join the edges before curing the shell inside of an elastomer balloon. Additional details and schematics regarding the simple fabrication process can be found in the **Supplementary Information** document.

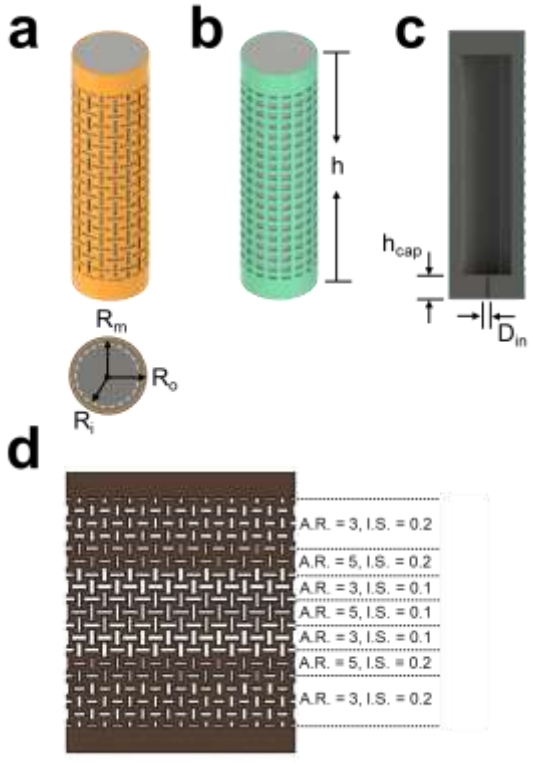


Figure 2: Concept design of extensile soft pneumatic actuators constructed from flexible center-symmetric perforated structures. Shown here are renderings of soft pneumatic actuators constructed using a TPU sheet with (a) *A.R.*=5, *I.S.*=0.1 and (b) *A.R.*=1, *I.S.*=0.2. A longitudinally sliced view of the actuator from (b) is shown in (c). An actuator is developed with a gradient sheet previously developed by the authors in Pagliocca *et al*.[16], which is presented along with the geometric details

Author Manuscript

This article is protected by copyright. All rights reserved

of unit cell geometries in (d). Panel (d) reproduced from CC-BY open access Elsevier publication, 2022.[16]

2.3. Free-Boundary Testing

We characterized the axial and radial expansion of the proposed soft robotic actuators through free-displacement boundary testing. These tests were performed to increase our understanding of the mechanical response of the actuators and provide ground for comparison with existing technologies. Prior to fabrication and testing, we constructed analytical models to predict the response of the actuators using the finite elastic methods of Connolly *et al*.[8] and Kassianidis[47] with modifications to restrict torsion and replace a homogenized anisotropic outer layer with an incompressible hyperelastic substitute. The analytical model presented in the **Supplementary Information** document was developed and validated to estimate the actuators' motions and required pressures for reasonable extensile actuation for design-of-experiment purposes (see **Figure S7** in the **Supplementary Information**). Our results predicted pressures around 50 kPa to achieve axial stretches of 0.15. These moderate stretches are restricted by localized unit cell deformation and reinforcement material properties. However, the same reinforcement structures offering only moderate axial deformation are later shown to offer unique advantages warranting their exploration.

Triplicate sets of actuators were fabricated and tested for each structure. We measured the applied pressure up to *ca*. 40 kPa and synchronously collected images to extract displacement measurements using the experimental setup and methods discussed in the **Supplementary Information** document. Averaged results are presented for axial and radial stretching of each extensile actuator in **Figure 3(a)** and **Figure 3(b)**, respectively. Motion coupling was investigated through the ratio of the axial stretch, λ_z, and radial stretch, λ_r, as presented in **Figure 3(c)**. Actuators with large axial motions and low radial motions are desirable.

Author Manuscript

This article is protected by copyright. All rights reserved

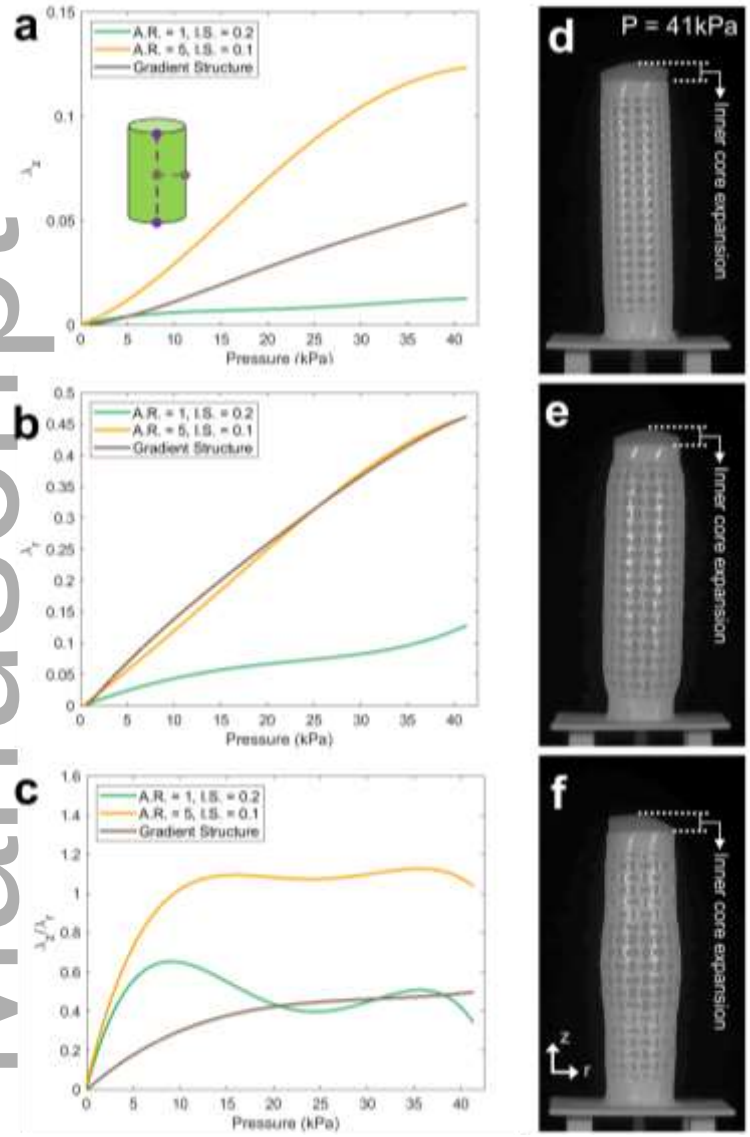


Figure 3: Free-boundary displacement experiments for each extensile actuator: (a) The mean axial stretch of the actuators. The vertical dashed line in the inset depicts the location of the axial stretch measurement, and the horizontal line shows that of the radial stretch. (b) The maximum radial stretch of the actuators, which occurs at the center of the actuator height in all tests. (c) The ratio between axial and radial stretches plotted against supplied pressure. Representative deformation images are shown for actuators with *A.R.*=1, *I.S.*=0.2 in (d), *A.R.*=5, *I.S.*=0.1 in (e), and the gradient structure in (f).

The actuators fabricated from sheets with *A.R.*=1, *I.S.*=0.2 exhibit the lowest axial and radial motions. Recalling the mechanics of the unit cells, the results are sensible as the high *A.R.* structures are mechanically more compliant. All actuators exhibit nonlinear response inherited from their hyperelastic constituent materials. Interestingly, actuators constructed from structures with a high *A.R.* have large motions at low pressure that abruptly plateau at higher pressures. Examining

This article is protected by copyright. All rights reserved

Author Manuscript

deformation images at 41 kPa in **Figure 3(d-f)**, we observed that unit cells approach rotation saturation, demonstrating that the mesomechanics of the reinforcement material indeed hold a high degree of influence on the response and tunability of the proposed soft robotic actuators. The latter point, *i.e.*, the tunability characteristics, can be further justified by examining the stretch ratios in **Figure 3(c)**. Comparing actuators with uniform cell designs, over 50 % improvement is obtained comparing the *A.R.*=5, *I.S.*=0.1 design over the *A.R.*=1, *I.S.*=0.2 counterpart. While it appears that higher *A.R.* designs have better motion decoupling, it is important to note that the larger motions are achieved at the cost of larger radial expansion, giving merit to the use of both high *A.R.* reinforcement structures and low *A.R.* reinforcement structures dependent on the application.

The actuators fabricated from the gradient structure display regions with large and small cell rotations as shown in **Figure 3(f)**. The gradient design shows improvements in increased axial displacements compared to the structure with *A.R.*=1, *I.S.*= 0.2. However, its performance is inferior compared with the actuators with *A.R.*=5, *I.S.*=1 design in the axial direction, while it shows a similar radial displacement response. It is worth noting here that this central region has a cell design with *A.R.*=5, *I.S.*=1, which is the same as the actuator in **Figure 3(e)**. The differences between the axial and radial motions indicate the circumferential stiffness is lower than the stiffness along the gradient. Further, the peak radial motions will closely resemble that of the most compliant layer, even in the presence of layers with different unit cell topologies. The obvious culprit of decreased axial response is the high stiffness layers in the gradient structure. However, the near-identical radial response suggests that the radial response is more effectively controlled by the most mechanically compliant (lowest stiffness region) and may be more spatially sensitive to the applied pressure. This result is advantageous because it suggests actuators designed for complex motions, like bending, should be governed by the mechanics of their most compliant layer, a topic investigated in later sections.

Upon examining the deformation images in **Figure 3(d-f)**, it is observed that the inner tube extends past the reinforcement region upon pressurization. With the application of high pressures, this extension can lead to significant differences in axial displacement if measured from the tip, as quantified in **Supplementary Information** document. This condition is clearly undesirable, particularly if the proposed modular soft robotic actuators are to be integrated into a system where positioning is critical. However, if the actuators are intended for a locomotive system or otherwise doing work on an object, the aforementioned condition may have a negligible effect on the structure's performance as the Ecoflex 00-50 material is several orders of magnitude more compliant than the structure as a whole (see **Supplementary Information**, Section 1). Further investigations of the role of a rigid confinement cap on the displacement of the topmost point of the structure are presented in **Supplementary Information**. These investigations suggest that the

This article is protected by copyright. All rights reserved

Author Manuscript

addition of a confinement cap has a negligible effect on the free response of the proposed actuators at the topmost point of the structure.

2.4. Confined-boundary and Efficiency Testing

We investigated the role of the reinforcement sleeve structures on the axial force exertion and the actuators' mechanical energy efficiency. To do so, practical benchmarks useful for possible future development of practical soft robotic systems were performed. To characterize the maximum force the extensile actuators can exert, we designed and implemented experiments where each actuator was inflated with a confined top boundary. Internal pressure, force, and images were collected synchronously. Data was recorded until an internal pressure of 70 kPa was achieved. We did not systematically explore the failure of these actuators. However, it is important to note that the actuators are most likely to fail under confined boundary conditions at the seam due to large radial expansions and stress concentration. Upon observation, this failure occurred at internal pressures far past the onset of mesoscale deformation-dominant behavior and was largely dependent on the quality of the seam where the reinforcement sheet was joined. Nonetheless, the failure behavior of the actuators was not characterized in the present study. Additional details regarding the experimental setup for confined top boundary testing can be found in the **Supplementary Information** document.

Averaged confined-boundary pressure-force results are presented in **Figure 4(a)**. Similar to the free-boundary tests, the actuators with an *A.R.*=5, *I.S.*=0.1 structure and those constructed from a gradient structure outperform the actuators constructed with the *A.R.*=1, *I.S.*=0.2 structure. Both the *A.R.*=5, *I.S.*=0.1 and gradient designs converge to a similar magnitude of force exertion, starting at around 35 kPa of an internal air pressure. Cylinders without a reinforcement structure were also tested with a confined top boundary. These structures exhibited poor performance compared to all reinforced designs and can be found in the **Supplementary Information** document. Up to a pressure of 35 kPa, the response of the gradient structured actuators is characterized by a notably larger generated axial force, which rapidly increases at low pressures. We attribute the increase in force in the gradient-structured actuators to the evolution of the large radial inflations within the center of the actuators. Specifically, as the center-most layers of the gradient structure actuators deform, the radial balloon will push the more rigid layers along the axial direction, generating higher forces. A small portion of the force is generated by the addition of equal and opposite reactions originating from deformation attributed to local cell rotations along the span of the cell density gradient acting in confinement, pushing the structural material towards the load cell while effectively transferring force between adjacent layers. To supplement this observation, we provide an image of a gradient actuator at high pressures (approximately 60 kPa) as an inset in **Figure 4(a)**.

This article is protected by copyright. All rights reserved

Author Manuscript

Similar behaviors are also present in the *A.R.*=5, *I.S.*=0.1 actuators. However, the force is less pronounced and effective, due to a smaller ballooning effect (*i.e.*, a smaller radius of balloon expanding outward). A larger number of similar unit cells along the axial direction results in more even distribution of local cell rotations, leading to a more uniform radial expansion of the actuator across its whole length.

Author Manuscript

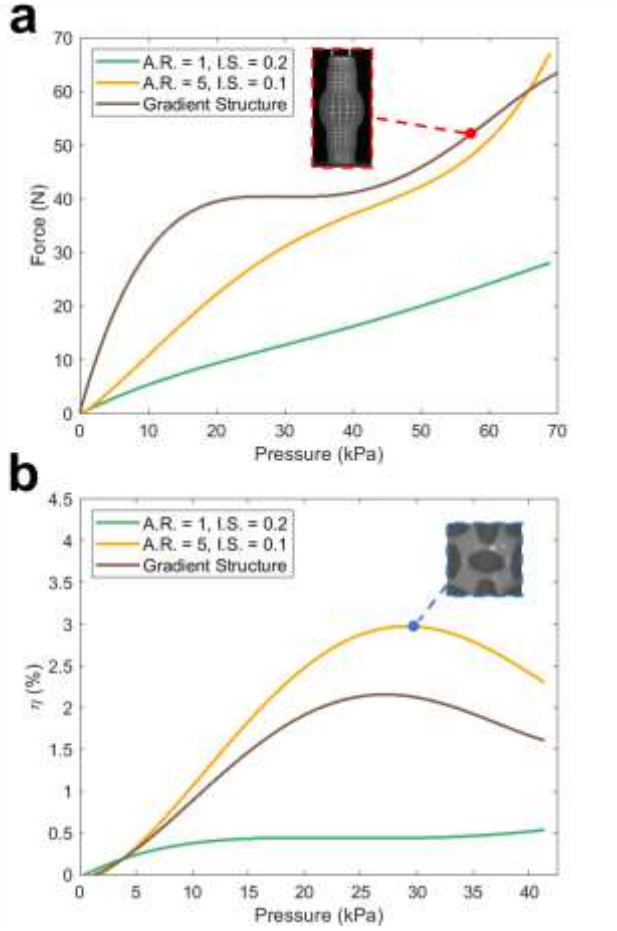


Figure 4: Mechanical response of extensile soft robotic actuators under an axially blocked tip condition, and while moving a fixed mass. (a) The pressure-force response upon pressurization with a confined top displacement boundary, with a snapshot of a gradient design actuator at high pressure shown as an inset. (b) Pressure-efficiency curves for each actuator from axial displacement tests of a fixed mass. The inset in (b) is from an *A.R.*=5, *I.S.*=0.1 actuator showing that peak efficiency occurs around local cell rotation saturation.

The mechanical energy efficiencies of the extensile actuators were characterized by determining the amount of work done by an actuator for measured input energy - see **Equation S20** in the **Supplementary Information** document.[48] An experimental apparatus is constructed to support a

This article is protected by copyright. All rights reserved

known mass (500 g) on a sliding mechanism that allows for simple extraction of the pressure-displacement measurements from captured images. The results of these analyses are presented in **Figure 4(b)**. Consistent with the pressure-displacement and pressure-force investigations, the *A.R.*=1, *I.S.*=0.2 structure actuators underperform the others. The actuator with the high *A.R.* structure shows the highest efficiency (*ca.* 3%) compared to the other two actuators. Our actuators were not optimized for efficiency and, thus, do perform less than those reported in the literature.[48] From a design perspective, a significant portion of energy losses can be attributed to width-wise expansion and friction at the bladder-reinforcement interface. It should be noted that width-wise expansion can be desirable, as was the case with actuators composed from the gradient structure with a confined boundary for exerting a higher force. In addition, the choice of sliding the reinforcement over the inner bladder simplifies the actuator construction and reduces the adverse effects of the unit cells wall material compressing the silicone while cells are rotating, in case the TPU lattice would have been molded inside the silicone rubber. Due to the large (>300×) difference in elastic moduli of TPU and Ecoflex 00-50, the expected losses due to the friction between the inner bladder and rotating cells are expected to be significantly smaller compared to the energy required for the cell rotation. Therefore, such losses were neglected here. Nonetheless, the high degree of friction at the interface between the silicone rubber and TPU hinders free cell rotation and offers significant room for efficiency improvement via modeling and improved materials selection. However, what is more important is the efficiency response of the *A.R.*=5, *I.S.*=0.1 and gradient structured actuators compared to the *A.R.*=1, *I.S.*= 0.2 actuators. The low *A.R.* actuators experience a plateau with a near-constant mechanical energy efficiency. On the other hand, the others which leverage local cell rotations experience clearly defined efficiency extrema. Examination of the deformation images shown as inset in **Figure 4(b)** reveals that the efficiency maxima occur near local cell rotation saturation, which as previously mentioned, is controlled by the local cell geometry. The latter observation indicates that the design of perforated structures for soft robotic applications required to exert positive work should focus on the identification of the transition between local rotation-dominant and deformation-dominant modes; this concept offers an opportunity for future research leading to shape optimizations.

2.5. Twisting, Bending, and Hybrid-motion Actuators

A benefit of using perforated structures in soft robotics lies in the local control of spatial stiffness of the reinforcement structures. Thus far, we have demonstrated the merits of such structures for applications as extensile actuators. Here, we expand the concept of local control of the structures' spatial stiffness to achieve bending, twisting, and hybrid motions. We develop structures to achieve these complex motions based on observation of the local deformations by drawing inspiration from

This article is protected by copyright. All rights reserved

Author Manuscript

the spatially variable axial and radial response demonstrated by the gradient design in previous sections. **Figure 5** provides schematics and characterizations of actuators with motions beyond extensile. **Figures 5(a,d)** present the bending actuator, **Figures 5(b,e)** the twisting actuator, and **Figures 5(c,f)** the hybrid bending-twisting actuators developed in this work. The unwrapped view of all perforated sheets is shown as insets in their respective motion-pressure curves. The perforated sheets used for these purposes were designed exclusively using the unit cells presented in **Figure 1**. At unit cell boundaries the larger void dimension is typically taken for perforations.

Bending structures were designed with low and high stiffness areas made with the unit cell designs of *A.R.*=5, *I.S.*=0.1 and *A.R.*=1, *I.S.*=0.2, respectively. The high stiffness area acts as a pseudo-inextensible layer similar to those used in pneumatic networks,[49] whereas the low stiffness areas can expand upon pressurization, causing the actuator to bend in a predefined programmed configuration. We call the stiff layer pseudo-inextensible because it deforms upon pressurization, but not to the same magnitude as the area with *A.R.*=5, *I.S.*=1, i.e., those that experience large deformations induced by local cell rotations. Upon inflation, the structural anisotropy and pseudo-inextensible layer leads to bending about the central axis of the cylindrical actuator as depicted in **Figure 5(a)-i**. We define the bending angle about the vertical axis of the actuator with the bending angle by the symbol β. The full-field deformation of the bending actuators is characterized using 3D (stereo) digital image correlation. The bending angles were measured at the topmost point of the reinforcement structure using the direction cosines. This is because the actuators do not bend perfectly perpendicular to the field of view. Additional experimental details can be found in the **Supplementary Information** document. The experimental results in **Figure 5(a,d)** show that the current unoptimized soft robotic actuator experiences moderate bending.

By carefully designing and placing the unit cells in our cylindrical reinforcement sheets, we developed soft actuators that can achieve twist. These twisting actuators draw their inspiration from fiber-reinforced soft pneumatic actuators,[8] where fibers are wound along the height of the actuator at a specific angle to achieve a desired trajectory. To achieve a similar effect, unit cells with *A.R.*=5, *I.S.*=1 were placed 45° apart by row on a planar sheet as shown in the inset (ii) of **Figure 5(b)**, prior to rolling into a cylinder. In this configuration, the solid portions resemble the fiber-reinforcement seen in a conventional twisting actuator. We measure the twist angle, θ, on a triplicate set of actuators using full-field measurements as shown in **Figure 5(b)**. The proposed twisting actuator can achieve small twists with an insignificant amount of axial extension as demonstrated in **Figure 5(b,e)**. The results of the achieved twist are substantial, demonstrating a potential for further performance enhancement by removing solid unit cells in the structure design.

Furthermore, to demonstrate the versatility of the proposed reinforcement structures for general soft robotics applications, we designed a perforated sheet that enables simultaneous bending

This article is protected by copyright. All rights reserved

Author Manuscript

and twisting as shown in **Figure 5(c)**. In this configuration, some extension is present as a consequence of pressurization as elucidated by the contour maps in **Figure 5(f)**. Triplicate sets of actuators were fabricated and tested using a combination of bending and twisting actuators. Results in **Figure 5(c)** and the strain contours in **Figure 5(f)** show that the actuator achieves both motions in unison, performing comparably to the individual sheets used to achieve bending or twisting. The improved twisting result originates as a result of the bending motion. Specifically, the tip bending projects further in the axis at which we measure twist, and not by greater strain accumulation in the layers designed to twist. The bending, however, is very comparable to that of the pure bending actuator (*i.e.*, **Figure 5(a)**). Recalling the radial deformation of the gradient structure, the out-of-plane motion tends to be controlled by the most mechanically compliant layer. We attain the same result here validating the dependence of radial motions on the local stiffness of the structure.

The results discussed in this section indicated that the spatial stiffness tuning method can be used to design and fabricate soft actuators whose cylindrical segments can achieve programmable twisting and bending motions. In addition, the actuators retain the capacity to achieve motions similar to the programmed balloons presented in Jin *et al*.[13] The notion of modularity can be exploited through individual perforation layers as shown in the hybrid motion actuators, or to develop actual modules that can be used to develop larger soft robotic actuators and arms as explored in the next section.

Author Manuscript

This article is protected by copyright. All rights reserved

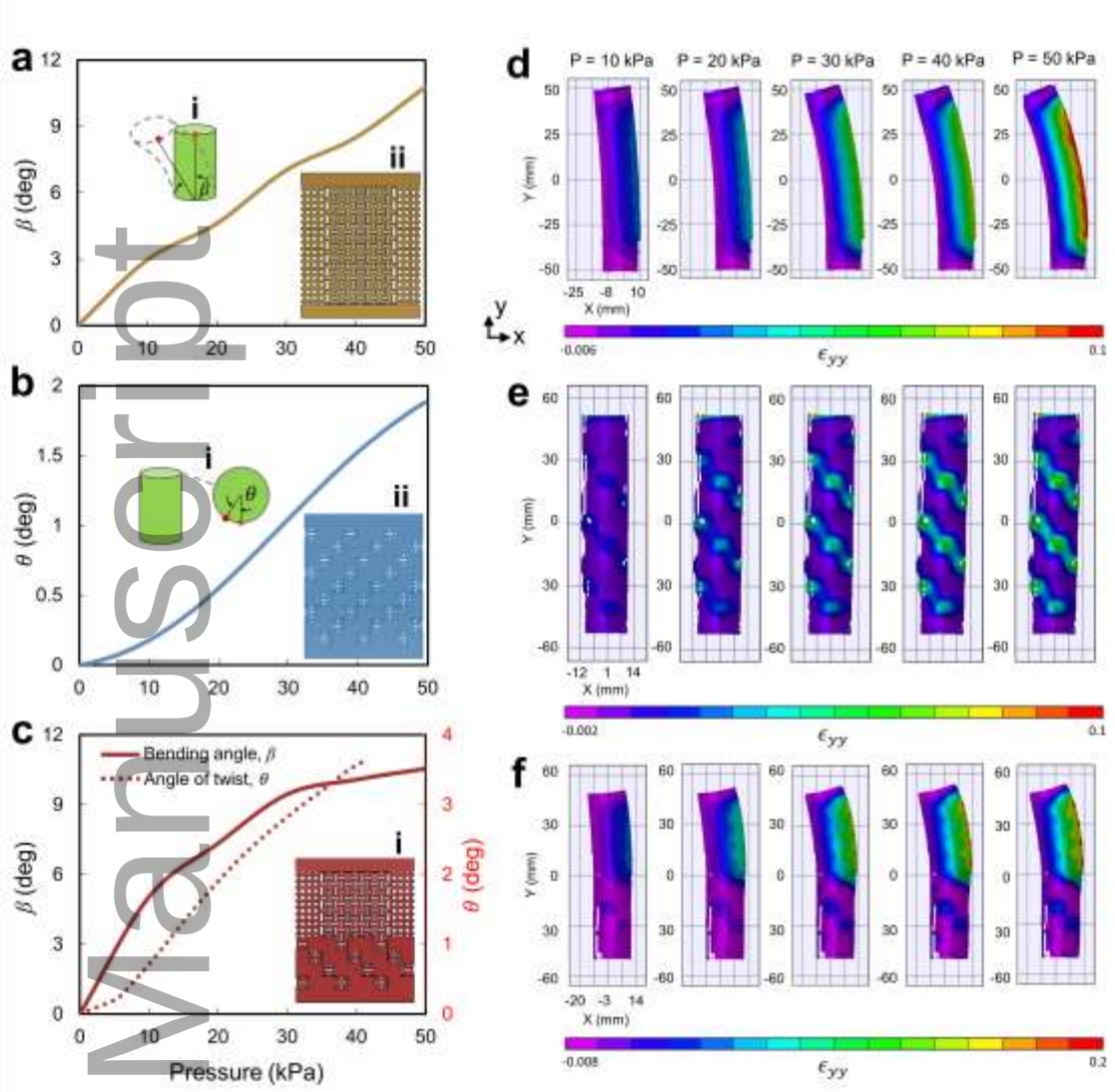


Figure 5: Soft robotic actuators that can achieve bending, twisting, and combined bend-twist motions. (a) The averaged response of the bending actuator with a schematic representation of the bending angle, β, in (a)-i and a schematic of the perforated sheet used in (a)-ii. (b) The averaged response of the twisting actuator with a schematic representation of the angle of twist, θ, presented in (b)-i and a schematic of the perforated sheet used in (b)-ii. (c) Results of the bending and twisting actuators used in the development of a hybrid bend-twist actuator with a schematic representation of its perforated sheet shown in (c)-i. Axial strain contours, ϵ_{yy}, are shown for representative bending, twisting, and hybrid bending-twisting actuators in (d), (e), and (f), respectively.

2.6. Multi-segment Configurations and Modular Soft Robotic Arms

The proposed actuators can be assembled to achieve complex spatial motions by joining several individual actuator segments together in series to bend, twist, extend, or utilize complex spatial motions in individual segments, thus constructing a segmented soft robotic arm. To prove this

This article is protected by copyright. All rights reserved

Author Manuscript

concept and demonstrate the utility of multi-segment configurations, we fabricated different actuators and assembled them in various configurations. For brevity, we only focus on a twisting-bending soft robotic arm configuration that naturally experiences extension, thus embodying all explored deformation modes in the study. The developed arm operated on a single air input. We joined segments together using the same fusing process used to fabricate the cylindrical sleeves from planar sheets and added an end cap to the most distal actuator. The same measurements and characterizations as in previous sections were performed. Discussions regarding the quantitative values of the complex motions are omitted, as we have already established the response of individual segments in earlier sections. Additional fabrication details of the multi-segment configurations can be found in the **Supplementary Information** document. We present deformation images of a twisting-bending multi-segment actuator in **Figure 6** at increasing pressures. From the results in the previous section, it may be argued that the same motions can be achieved using a single sheet of sufficient height. However, the results of connecting multiple segments in series were intentionally chosen to further demonstrate the concept that the actuators can be easily scaled up with simple connection methods, by leveraging the thermoplastic properties of the reinforcement structure. It is of similar utility to develop formal connectors to achieve the same effect to realize large and scalable soft robotic actuators and systems.

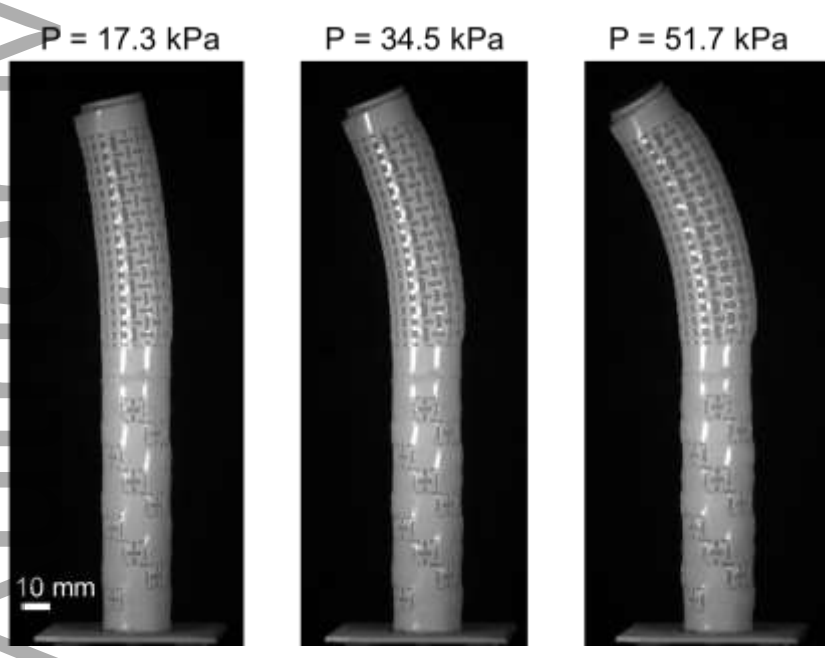


Figure 6: Deformation image sequence of a multi-segment twisting-bending actuator at different internal pressures.

Our work bridges materials and robotics engineering through the development of novel soft robotic actuators and arms with programmable deformations and mechanical responses. The

This article is protected by copyright. All rights reserved

Author Manuscript

proposed single actuators can be programmed for specific displacement/motion and force exertion characteristics, and naturally for optimal mechanical energy efficiency. The key to unlocking the full potential of the methodology lies in the local identification of cell rotation saturation in a multi-axial stress state, as this marks the onset of deformation plateaus in all actuators. As discussed in the **Supplementary Information** document, the analytical model for the extensile actuators presented therein can be further extended to characterize the complex motions and interactions of single actuators, with the potential of further extension to capture bending and twisting motions. It remains a topic of future research to optimize these structures for use in practical soft robotic actuators. Both individual actuators and soft robotic arms assembled from multiple actuators could be used as versatile grippers to interact with delicate objects, such as glass containers or food, to mimic shapes, or manifest themselves as elements of larger robotic systems in the form of compliant links. Specifically, the kinematic shape changes such as change of radius can enable grasping of cylindrical elements (e.g., cups or vases) from the interior. Improved modeling and simulation will enable such investigations. Here, we focused on a multi-scale mechanics approach exclusively to establish a foundation for improved designs and future research. We selected base unit cells exclusively based on the characteristics of their planar deformation modes (auxetic vs. non-auxetic). Further, we restricted ourselves to not removing unit cells, but instead, altering the local mechanical stiffness by unit cell design. Based on the experimental results obtained, we find that it is not only possible to control the magnitude of the applied force, but one can also control how effectively the force is applied based on the local tuning of the radial ballooning. The same mechanisms used therein allow for the design of non-axial motions such as bending with minimal rows and number of unit cells. The modular nature of our actuators enables the construction of a versatile class of soft robotic systems achievable with flexible perforated materials.

Supporting Information

Additional details regarding sample fabrication, design of experiments, analytical modeling, and raw data collection are presented as Supplementary Information.

Acknowledgments

This material is based upon work supported by the National Science Foundation under Grant No. 2035660 (B.K.). B.K. acknowledges the Advanced Materials and Manufacturing Institute (AMMI) at Rowan University for partial financial support of the project.

Author Manuscript

This article is protected by copyright. All rights reserved

Received: ((will be filled in by the editorial staff))
Revised: ((will be filled in by the editorial staff))
Published online: ((will be filled in by the editorial staff))

Author Manuscript

References

[1] J. Luong, P. Glick, A. Ong, M. S. deVries, S. Sandin, E. W. Hawkes, and M. T. Tolley, "Eversion and retraction of a soft robot towards the exploration of coral reefs," in 2019 2nd IEEE International Conference on Soft Robotics (RoboSoft), pp. 801–807, 2019.

[2] P. Polygerinos, N. Correll, S. A. Morin, B. Mosadegh, C. D. Onal, K. Petersen, M. Cianchetti, M. T. Tolley, and R. F. Shepherd, "Soft Robotics: Review of fluid-driven intrinsically soft devices; manufacturing, sensing, control, and applications in human-robot interaction," Advanced Engineering Materials, vol. 19, no. 12, 2017.

[3] L. Wang, G. Peng, W. Yao, S. Biggar, C. Hu, X. Yin, and Y. Fan, "Soft robotics for hand rehabilitation," in Intelligent Biomechatronics in Neurorehabilitation, pp. 167–176, 2019.

[4] M. Raeisinezhad, N. Pagliocca, B. Koohbor, and M. Trkov, "Design optimization of a pneumatic soft robotic actuator using model-based optimization and deep reinforcement learning," Frontiers in Robotics and AI, vol. 8, 2021.

[5] S. Cai, C. Tang, L. Pan, G. Bao, W. Bai, and Q. Yang, "Pneumatic webbed soft gripper for unstructured grasping," International Journal of Agricultural and Biological Engineering, vol. 14, no. 4, pp. 145–151, 2021.

[6] B. T. Phillips, K. P. Becker, S. Kurumaya, K. C. Galloway, G. Whittredge, D. M. Vogt, C. B. Teeple, M. H. Rosen, V. A. Pieribone, D. F. Gruber, and R. J. Wood, "A dexterous, glove-based teleoperable low-power soft robotic arm for delicate deep-sea biological exploration," Scientific Reports, vol. 8, no. 1, pp. 14779–9, 2018.

[7] B. Gorissen, D. Reynaerts, S. Konishi, K. Yoshida, J. Kim, and M. De Volder, "Elastic inflatable actuators for soft robotic applications," Advanced Materials, vol. 29, no. 43, pp. 1604977, 2017.

[8] F. Connolly, C. J. Walsh, and K. Bertoldi, "Automatic design of fiber-reinforced soft actuators for trajectory matching," Proceedings of the National Academy of Sciences - PNAS, vol. 114, no. 1, pp. 51–56, 2017.

[9] M. Schaffner, J. A. Faber, L. Pianegonda, P. A. R¨uhs, F. Coulter, and A. R. Studart, "3D printing of robotic soft actuators with programmable bioinspired architectures," Nature Communications, vol. 9, no. 1, pp. 878–9, 2018.

This article is protected by copyright. All rights reserved

[10] J. Walker, T. Zidek, C. Harbel, S. Yoon, F. S. Strickland, S. Kumar, and M. Shin, "Soft robotics: A review of recent developments of pneumatic soft actuators," Actuators, vol. 9, no. 1, pp. 3–, 2020.
[11] N. El-Atab, R. B. Mishra, F. Al-Modaf, L. Joharji, A. A. Alsharif, H. Alamoudi, M. Diaz, N. Qaiser, and M. M. Hussain, "Soft actuators for soft robotic applications: A review," Advanced Intelligent Systems, vol. 2, no. 10, pp. 2000128–n/a, 2020.
[12] T. J. Jones, E. Jambon-Puillet, J. Marthelot, and P.-T. Brun, "Bubble casting soft robotics," Nature, vol. 599, no. 7884, pp. 229–233, 2021.
[13] L. Jin, A. E. Forte, B. Deng, A. Rafsanjani, and K. Bertoldi, "Kirigami-inspired inflatables with programmable shapes," Advanced Materials, vol. 32, no. 33, pp. 2001863–n/a, 2020.
[14] J. N. Grima and R. Gatt, "Perforated sheets exhibiting negative Poisson's ratios," Advanced Engineering Materials, vol. 12, no. 6, pp. 460–464, 2010.
[15] K. Bertoldi, P. M. Reis, S. Willshaw, and T. Mullin, "Negative Poisson's ratio behavior induced by an elastic instability," Advanced materials (Weinheim), vol. 22, no. 3, pp. 361–366, 2010.
[16] N. Pagliocca, K. Z. Uddin, I. A. Anni, C. Shen, G. Youssef, and B. Koohbor, "Flexible planar metamaterials with tunable Poisson's ratios," Materials and Design, vol. 215, pp. 110446–, 2022.
[17] J. N. Grima, R. Gatt, B. Ellul, and E. Chetcuti, "Auxetic behaviour in non-crystalline materials having star or triangular shaped perforations," Journal of Non-Crystalline Solids, vol. 356, no. 37, pp. 1980–1987, 2010.
[18] J. N. Grima and K. E. Evans, "Auxetic behavior from rotating squares," Journal of Materials Science Letters, vol. 19, no. 17, pp. 1563–1565, 2000.
[19] L. Mizzi, E. Mahdi, K. Titov, R. Gatt, D. Attard, K. E. Evans, J. N. Grima, and J.-C. Tan, "Mechanical metamaterials with star-shaped pores exhibiting negative and zero Poisson's ratio," Materials and Design, vol. 146, pp. 28–37, 2018.
[20] K. Billon, I. Zampetakis, F. Scarpa, M. Ouisse, E. Sadoulet-Reboul, M. Collet, A. Perriman, and A. Hetherington, "Mechanics and band gaps in hierarchical auxetic rectangular perforated composite metamaterials," Composite Structures, vol. 160, pp. 1042–1050, 2017.
[21] J. N. Grima, L. Mizzi, K. M. Azzopardi, and R. Gatt, "Auxetic perforated mechanical metamaterials with randomly oriented cuts," Advanced Materials, vol. 28, no. 2, pp. 385–389, 2016.
[22] J. Yao, Y. Su, F. Scarpa, and Y. Li, "An optimization approach to design deformation patterns in perforated mechanical metamaterials using distributions of Poisson's ratio-based unit cells," Composite Structures, vol. 281, pp. 115015–, 2022.

This article is protected by copyright. All rights reserved

Author Manuscript

[23] J. K. Wilt, C. Yang, and G. X. Gu, "Accelerating auxetic metamaterial design with deep learning," Advanced Engineering Materials, vol. 22, no. 5, pp. 1901266–n/a, 2020.
[24] W. Zhang, Z. Li, J. Wang, F. Scarpa, and X. Wang, "Mechanics of novel asymmetrical re-entrant metamaterials and metastructures," Composite Structures, vol. 291, pp. 115604–, 2022.
[25] M. Lei, W. Hong, Z. Zhao, C. Hamel, M. Chen, H. Lu, and H. J. Qi, "3D printing of auxetic metamaterials with digitally reprogrammable shape," ACS applied materials interfaces, vol. 11, no. 25, pp. 22768–22776, 2019.
[26] A. Rafsanjani, L. Jin, B. Deng, and K. Bertoldi, "Propagation of pop ups in kirigami shells," Proceedings of the National Academy of Sciences - PNAS, vol. 116, no. 17, pp. 8200–8205, 2019.
[27] X. Xin, L. Liu, Y. Liu, and J. Leng, "4D printing auxetic metamaterials with tunable, programmable, and reconfigurable mechanical properties," Advanced Functional Materials, vol. 30, no. 43, 2020.
[28] R. L. Truby, L. Chin, and D. Rus, "A recipe for electrically-driven soft robots via 3d printed handed shearing auxetics," IEEE robotics and automation letters, vol. 6, no. 2, pp. 795–802, 2021.
[29] R. Hedayati, A. G¨uven, and S. van der Zwaag, "3d gradient auxetic soft mechanical metamaterials fabricated by additive manufacturing," Applied Physics Letters, vol. 118, no. 14, 2021.
[30] A. Lazarus and P. M. Reis, "Soft actuation of structured cylinders through auxetic behavior: Soft actuation of structured cylinders through," Advanced Engineering Materials, vol. 17, no. 6, pp. 815–820, 2015.
[31] F. Javid, J. Liu, J. Shim, J. C. Weaver, A. Shanian, and K. Bertoldi, "Mechanics of instability induced pattern transformations in elastomeric porous cylinders," Journal of The Mechanics and Physics of Solids, vol. 96, pp. 1–17, 2016.
[32] D. Yang, B. Mosadegh, A. Ainla, B. Lee, F. Khashai, Z. Suo, K. Bertoldi, and G. M. Whitesides, "Buckling of elastomeric beams enables actuation of soft machines," Advanced Materials, vol. 27, no. 41, pp. 6323–6327, 2015.
[33] D. Yang, M. S. Verma, J. So, B. Mosadegh, C. Keplinger, B. Lee, F. Khashai, E. Lossner, Z. Suo, and G. M. Whitesides, "Buckling pneumatic linear actuators inspired by muscle," Advanced Materials Technologies, vol. 1, no. 3, pp. 1600055–n/a, 2016.
[34] A. Sedal, M. Fisher, J. Bishop-Moser, A. Wineman, and S. Kota, "Auxetic sleeves for soft actuators with kinematically varied surfaces," in 2018 IEEE/RSJ International Conference on Intelligent Robots and Systems (IROS), pp. 464–471, IEEE, 2018.
[35] A. Sedal, J. Bishop Moser, S. Kota, M. Fisher, M. Kohler, and A. Wineman, "Fluidic actuator system using auxetic beam reinforcements," U.S. Patent 11,255,356 B2, Feb. 22, 2022.

This article is protected by copyright. All rights reserved

Author Manuscript

[36] M. F. Simons, K. M. Digumarti, A. T. Conn, and J. Rossiter, “Tiled auxetic cylinders for soft robots,” in 2019 2nd IEEE International Conference on Soft Robotics (RoboSoft), pp. 62–67, IEEE, 2019.
[37] N. Pagliocca, “Design and control of modular soft robotic actuators with architected structures,” Master’s thesis, Rowan University, 2022.
[38] C. Branyan, A. Rafsanjani, K. Bertoldi, R. L. Hatton, and Y. Meng¨u¸c, “Curvilinear kirigami skins let soft bending actuators slither faster,” Frontiers in robotics and AI, vol. 9, pp. 872007–872007, 2022.
[39] S. Joe, M. Totaro, and L. Beccai, “Analysis of soft kirigami unit cells for tunable stiffness architectures,” in 2021 IEEE 4th International Conference on Soft Robotics (RoboSoft), pp. 343–350, IEEE,
2021.
[40] B. Liu, Y. Ozkan-Aydin, D. I. Goldman, and F. L. Hammond, “Kirigami skin improves soft earthworm robot anchoring and locomotion under cohesive soil,” in 2019 2nd IEEE International Conference on Soft Robotics (RoboSoft), pp. 828–833, IEEE, 2019.
[41] H. Khosravi, S. M. Iannucci, and S. Li, “Pneumatic soft actuators with kirigami skins,” Frontiers in Robotics and AI, vol. 8, pp. 749051–749051, 2021.
[42] R. L. Truby, C. D. Santina, and D. Rus, “Distributed proprioception of 3d configuration in soft, sensorized robots via deep learning,” IEEE Robotics and Automation Letters, vol. 5, no. 2, pp. 3298– 3305, 2020.
[43] L. J. Gibson and M. F. Ashby, Cellular Solids: Structure and Properties. Cambridge Solid State Science Series, Cambridge University Press, 2 ed., 1997.
[44] O. Rahman and B. Koohbor, “Optimization of energy absorption performance of polymer honeycombs by density gradation,” Composites Part C: Open Access, vol. 3, pp. 100052–, 2020.
[45] I. A. Anni, K. Z. Uddin, N. Pagliocca, N. Singh, O. Rahman, G. Youssef, and B. Koohbor, “Out-of-plane load-bearing and mechanical energy absorption properties of flexible density-graded TPU honeycombs,” Composites Part C: Open Access, vol. 8, pp. 100284–, 2022.
[46] K. Uddin, N. Pagliocca, I. Anni, G. Youssef, and B. Koohbor, “Multiscale strain field characterization in flexible planar auxetic metamaterials with rotating squares,” Advanced Engineering Materials, vol. 25, no. 2, pp. 2201248, 2023.
[47] F. Kassianidis, Boundary-value problems for transversely isotropic hyperelastic solids. Ph.D. thesis, University of Glasgow, 2007.
[48] S. Li, D. M. Vogt, D. Rus, and R. J. Wood, “Fluid-driven origami-inspired artificial muscles,” Proceedings of the National Academy of Sciences, vol. 114, no. 50, pp. 13132–13137, 2017.

Author Manuscript

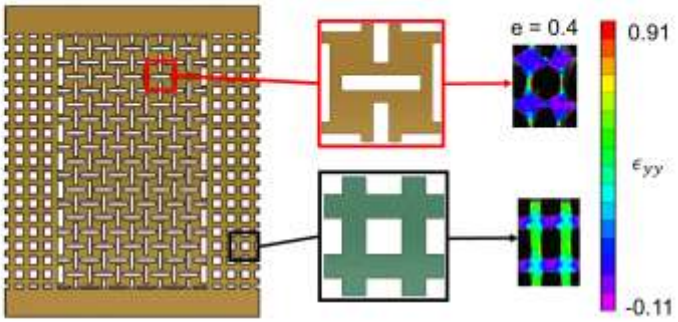
This article is protected by copyright. All rights reserved

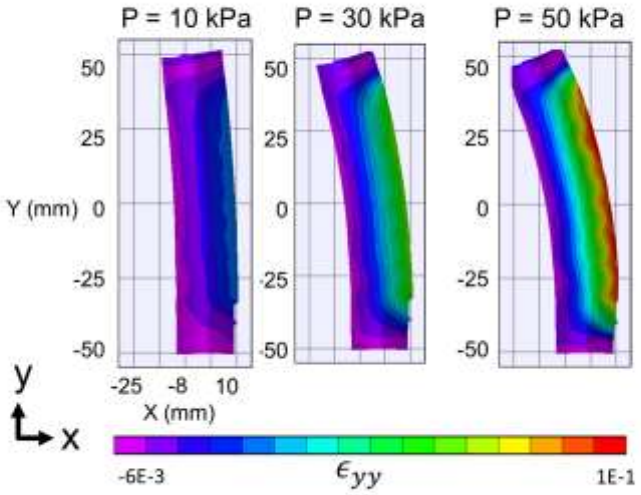
[49] B. Mosadegh, P. Polygerinos, C. Keplinger, S. Wennstedt, R. F. Shepherd, U. Gupta, J. Shim, K. Bertoldi, C. J. Walsh, and G. M. Whitesides, "Pneumatic networks for soft robotics that actuate rapidly," Advanced Functional Materials, vol. 24, no. 15, pp. 2163–2170, 2014.

Table of Contents

Modular soft robotic actuators are designed by carefully tuning the spatial stiffness of a flexible reinforcement structure at the mesoscale. The utility of the proposed methodology is first demonstrated by controlling the deformations, force-exertion, and quantifying the energy efficiency of extensile actuators. The design concepts are extended to the development of actuators with programmable complex motions.







This article is protected by copyright. All rights reserved